HHS Public Access

Author manuscript

Exp Hematol. Author manuscript; available in PMC 2020 November 18.

Published in final edited form as:

Exp Hematol. 2020 August ; 88: 42–55. doi:10.1016/j.exphem.2020.07.001.

TLR2/6 signaling promotes the expansion of premalignant hematopoietic stem and progenitor cells in the *NUP98-HOXD13* mouse model of MDS

Darlene A. Monlish[a], **Zev J. Greenberg**[a], **Sima T. Bhatt**[a], **Kathryn M. Leonard**[a], **Molly P. Romine**[a], **Qian Dong**[a], **Lauren Bendesky**[a], **Eric J. Duncavage**[b], **Jeffrey A. Magee**[a], **Laura G. Schuettpelz**[a]

[a]Department of Pediatrics, Washington University School of Medicine, St. Louis, MO;

[b]Department of Pathology and Immunology, Washington University School of Medicine, St. Louis, MO

Abstract

Toll-like receptor 2 (TLR2) expression is increased on hematopoietic stem and progenitor cells (HSPCs) of patients with myelodysplastic syndromes (MDS), and enhanced TLR2 signaling is thought to contribute to MDS pathogenesis. Notably, TLR2 heterodimerizes with TLR1 or TLR6, and while high TLR2 is associated with lower-risk disease, high TLR6, but not TLR1, correlates with higher-risk disease. This raises the possibility of heterodimer-specific effects of TLR2 signaling in MDS, and in the work described here, we tested the effects of specific modulation of TLR1/2 versus TLR2/6 signaling on premalignant HSPCs. Indeed, chronic stimulation of TLR2/6, but not TLR1/2, accelerates leukemic transformation in the *NHD13* mouse model of MDS, and conversely, loss of TLR6, but not TLR1, slows this process. TLR2/6 stimulation expands premalignant HSPCs, and chimeric mouse studies revealed that cell-autonomous signaling contributes to this expansion. Finally, TLR2/6 stimulation is associated with an enrichment of Myc and mTORC1 activities. While Myc inhibition partially suppressed the TLR2/6 agonist-mediated expansion of premalignant HSPCs, inhibition of mTORC1 exacerbated it, suggesting that these pathways play opposite roles in regulating the effects of TLR2/6 ligation on HSPCs. Together, these data reveal heterodimer-specific effects of TLR2 signaling on premalignant HSPCs, with TLR2/6 signaling promoting their expansion and leukemic transformation.

The myelodysplastic syndromes are a group of hematopoietic stem and progenitor cell (HSPC) disorders characterized by abnormal hematopoiesis and a high risk of transformation to acute leukemia [1,2]. Numerous prior studies have described enhanced

Offprint requests to: Laura G. Schuettpelz, Department of Pediatrics, Washington University School of Medicine, 660 South Euclid Ave, St. Louis, MO 63110; Schuettpelz_l@wustl.edu.

DAM, ZJG, STB, KML, MPR, QD, LB, JAM, and LGS performed experiments and analyzed data. EJD reviewed all pathology. LGS directed the study. DAM, ZJG, and LGS wrote and edited the article.

Conflict of interest disclosure

The authors declare no conflicts of interest.

Supplementary material associated with this article can be found in the online version at https://doi.org/10.1016/j.exphem.2020.07.001.

innate immune signaling and, in particular, increased toll-like receptor (TLR) signaling in the CD34+ stem and progenitor cells of patients with MDS [3–11]. This enhanced TLR signaling is thought to contribute to the ineffective hematopoiesis and cell death that are prominent features of lower-risk disease [12]. Among the TLR family members, RNA levels of TLR2 have been reported to be increased in the majority of patients with MDS, with the highest expression in patients with low-risk disease, by International Prognostic Scoring System [3,11]. Given its pervasive overexpression and the fact that chronic TLR stimulation is known to impair normal hematopoietic stem cell function [13–16], TLR2 is an attractive therapeutic target for patient with MDS [17]; however, its role in the disease remains unclear.

To study the role of TLR2 signaling in MDS, we used the *NUP98-HOXD13* (*NHD13*) mouse model. This well-characterized transgenic MDS model expresses the *NUP98-HOXD13* fusion from the hematopoietic Vav-1 promoter and exhibits many of the salient features of human MDS including cytopenias, bone marrow dysplasia, and transformation to acute leukemia [18]. Notably, the HSPCs of the NHD13 mice, like those of humans with MDS, have increased expression of TLR2, and we recently reported that complete loss of TLR2 or the TLR signaling adaptor MyD88 is associated with earlier leukemic transformation in the *NHD13* mice [19]. Mechanistic studies revealed that loss of TLR2 resulted in a reduction of activated caspase-1 and lower rates of cell death in preleukemic HSPCs [19]. Together, these data suggest that some TLR signaling may be protective against the progression of MDS to acute leukemia, and are consistent with patient data indicating that high TLR2 expression correlates with lower-risk disease and better overall survival [3,11]. TLR2 functions largely as a heterodimer with TLR1 or TLR6, and notably, while high TLR2 is associated with lower-risk disease, high TLR6 correlates with higher-risk disease and a trend toward poorer survival [3]. This raises the intriguing possibility that there are heterodimer-specific effects of TLR2 signaling in MDS pathogenesis, and herein we used the *NHD13* mouse model to test the effects of specific modulation of TLR1/2 versus TLR2/6 signaling on premalignant HSPCs. Indeed, we find that chronic treatment of *NHD13* mice with a TLR2/6 agonist, but not a TLR1/2 agonist, leads to more robust cycling and expansion of HSPCs, and accelerates the development of leukemia and death. Conversely, loss of TLR6, but not TLR1, extends survival of the *NHD13* mice. TLR2/6 agonist treatment is associated with a marked increase in serum interleukin (IL)-6; however, loss of IL-6 did not mitigate the TLR2/6 agonist-specific expansion of HSPCs. Rather, chimeric mouse studies suggested that the TLR2/6 agonist-mediated effects on premalignant HSPCs are, at least in part, cell autonomous. Finally, RNA profiling studies found that TLR2/6 stimulation is associated with enrichment of Myc and mTORC1 targets. Myc inhibition partially mitigated the TLR2/6 agonist-mediated expansion of premalignant HSPCs. Conversely, mTORC1 inhibition resulted in a dramatic exacerbation of the TLR2/6 agonist-mediated HSPC expansion in *NHD13* mice, suggesting that Myc and mTORC1 have opposite roles in mediating the effects of TLR2/6 stimulation on premalignant HSPCs. Collectively, these data reveal that there are indeed heterodimer-specific effects of TLR2 signaling on premalignant HSPCs, with TLR2/6 stimulation, but not TLR1/2 stimulation, promoting HSPC expansion and leukemogenesis in the *NHD13* mouse model.

Methods

Mice

C57BL/6J, C57BL/6 (B6.SJL-Ptprc^{a} Pepc^{b}/BoyJ; CD45.1), *NUP98-HOXD13* (C57BL/6-Tg(Vav1-NUP98/HOXD13)G2-Apla/J), *Il-6*$^{-/-}$ (B6.129S2-Il6^{tm1Kopf}/J), and *Tlr1*$^{-/-}$ (B6.129S1-Tlr1^{tm1Flv}/J) mice were obtained from the Jackson Laboratory (Bar Harbor, ME). *Tlr6*$^{-/-}$ mice were obtained from Oriental BioService, Inc. (Kyoto, Japan). All mice were maintained on a C57BL/6J background. Sex- and age-matched mice were used in accordance with the guidelines of the Washington University Animal Studies Committee.

TLR2 agonist and inhibitor injections

PAM_3CSK_4 and PAM_2CSK_4 (InvivoGen, San Diego, CA) were reconstituted in sterile water and delivered by intraperitoneal (IP) injection. Unless otherwise indicated, mice were administered 1 μg PAM_2CSK_4, 25 μg PAM_3CSK_4, or water (vehicle) per dose, 3 doses/week, for the duration of the study. For short-term treatment regimens, the final dose was administered 24 hours before euthanization. For JQ1 treatments, mice were administered 1 mg JQ1 via IP injection 2 hours before TLR2 agonist treatment [20]. JQ1 (Adooq Bioscience, Irvine, CA)was prepared as a 50 mg/mL stock in DMSO, then diluted to 5 mg/mL with 10% 2-hydroxypropyl-β-cyclodextrin. For rapamycin treatments, mice were administered 0.15 mg rapamycin IP daily (dissolved in 2% dimethyl sulfoxide [DMSO], 30% polyethylene glycol [PEG] 300, and 5% Tween 80 in double-distilled water; Selleck Chemicals, Houston, TX).

Western blotting

Thirty thousand KSL cells were sorted into 10% trichloroacetic acid, pelleted at 14,000 rpm for 10 min at 4°C, and washed twice with acetone. Dried pellets were resuspended in solubilization buffer (9 mol/L urea, 2% Triton X-100, and 1% dithiothreitol [DTT]), and incubated with loading dye at 70°C for 10 min. Samples were run on 4%–12% Bis-Tris Plus Gels (Invitrogen, Carlsbad, CA) and transferred to poly-vinyl difluoride (PVDF) membranes. Membranes were probed for phospho-STAT1 (No. 9167, Cell Signaling, Danvers), STAT1 (No. 9172, Cell Signaling), pErk1/2 (No. 4370, Cell Signaling), Erk1/2 (No. 4696, Cell Signaling), and rabbit anti-mouse HRP-conjugated secondary antibody (No. 7074, Cell Signaling). Proteins were detected using Pierce ECL Western Blotting Substrate (ThermoFisher, Kalamazoo, MI) on chemiluminescence film.

Survival study mouse analysis

Moribund mice were euthanized, and 1×10^6 bone marrow or spleen cells and 100 μL of blood cells were prepared in 200 μL of fluorescence-activated cell sorting (FACS) buffer supplemented with bovine serum albumin (A10008–01, Gibco, Gaithersburg, MD). The cells were spun onto glass slides using a Shandon Cytospin 3 (8 min at 500 rpm) and stained using Protocol Hema 3 Wright-Giemsa stain (ThermoFisher). Images were captured with an Axioskop 2 micro-scope equipped with an Axiocam camera and Zen software (Carl Zeiss Microscopy, LLC, Thornwood, NY). Cells were also prepared and stained for flow

cytometry using the antibodies under Supplementary Data (online only, available at www.exphem.org).

Flow cytometry

Blood was obtained by retro-orbital sampling. Bone marrow cells were isolated by centrifugation of femurs at 6,000 rpm for 3 min [21]. Spleen cells were harvested by being crushed through a 100 μmol/L strainer. Cells were processed for staining as previously described [22] and stained using the antibodies listed in the Supplementary Data. Cell counts were determined using the Hemavet HV950 (Drew Scientific, Miami Lake, FL). Stained cells were analyzed on a Gallios flow cytometer (Beckman Coulter, Indianapolis, IN). Data were analyzed with FlowJo software (version 10.5.3, TreeStar, Ashland, OR).

Cell cycle analysis

Bone marrow cells were stained for surface markers (see Supplementary Data), fixed using the BD Cytofix/Cytoperm Kit (BD Biosciences, Franklin Lakes, NJ), blocked with 5% goat serum, stained with mouse anti-human Ki-67 (clone B56, BD Pharmingen) per the manufacturer's instructions, washed, and resuspended in 4′,6-diamidino-2-phenylindone (DAPI)-containing FACS buffer.

Cell death analysis

Bone marrow cells were stained for surface markers (Supplementary Data) and then washed in 1 × binding buffer, and 2×10^6 cells were stained with the Annexin V Apoptosis Detection Kit APC (ThermoFisher) before flow cytometry analysis.

Cell sorting

Bone marrow cells were obtained by crushing bones in phosphate-buffered saline supplemented with 2% bovine serum albumin. Single-cell suspensions were filtered using a 40-μm filter before staining with antibodies (see Supplementary Data) on ice for 20 min. c-Kit+ cells were pre-enriched before sorting on a BD FACSAria Fusion (BD Biosciences) by selection with biotin-conjugated paramagnetic beads using the MACS Separator (Miltenyi Biotec, Auburn, CA). Nonviable cells were excluded by DAPI staining.

MethoCult serial replating assays

One thousand KSL cells were sorted into 300 μL of FACS buffer supplemented with 2% bovine serum albumin, then transferred to 3 mL of MethoCult GF M3434 (Stem Cell Technologies, Vancouver, BC, Canada) and plated onto 35 × 10-mm Petri dishes in duplicate. Colonies were scored after 7 days of growth at 37°C in a humidified chamber with 5% CO_2. Cells were then collected, pooled, and replated at a density of 1×10^3 cells per well.

Transplantation of sorted KSL cells

For transplantation studies of cells from treated *NHD13* mice, 1×10^3 KSL cells were sorted and transplanted into sublethally irradiated (250 cGy) wild-type (WT; CD45.1) mice.

Cytokine analysis

Mice were treated with a single dose of TLR agonist. After 4 hours, blood was obtained via cardiac puncture, allowed to clot at room temperature for 1–2 hours, and then centrifuged for 10 min at 6,000 rpm. Serum was assessed using the Proteome Profiler Mouse Cytokine Array Kit (R&D Systems, Minneapolis, MN), according to the manufacturer's instructions. Densitometry was performed using ImageJ (National Institutes of Health, Bethesda, MD). For IL-6 measurements, serum was assessed using the mouse IL-6 Quantikine ELISA kit (R&D Systems).

Chimera generation

Chimeric mice were generated by transplanting a 1:1 mixture of whole bone marrow cells from *NHD13* mice (CD45. 1/CD45.2) with bone marrow from *NHD13;Tlr2*$^{-/-}$ or *NHD13;Tlr6*$^{-/-}$ mice (CD45.2) into lethally irradiated WT (CD45.1) recipients. CD45.1/CD45.2 *NHD13* mice were generated by crossing *NHD13* (CD45.2) mice with C57BL/6 (B6.SJL-Ptprc*Pep3bBoyJ) mice to generate CD45.1/CD45.2 *NHD13* mice. A total of 2×10^6 cells was transplanted via retro-orbital injection into lethally irradiated (two doses of 550 cGy) WT CD45.1 mice. Cells were allowed to engraft for at least 12 weeks before further analysis.

Gene expression array analysis

RNA was prepared from sorted KSL cells using NucleoSpin RNA XS (Macherey-Nagel, Bethlehem, PA), amplified using the Sigma Complete Whole Transcriptome Amplification Kit (WTA2, Millipore Sigma, Darmstadt, Germany), and analyzed using the Agilent Mouse Gene Expression v2 8 × 60K Microarray (Agilent). Gene set enrichment analysis (GSEA) was performed using the GSEA software (Broad Institute).

Statistical analysis

Data are presented as mean ± SEM, unless otherwise stated. Statistical significance was assessed using an unpaired, two-tailed Student *t* test or the Log-rank (Mantel-Cox) test. GraphPad Prism (version 8.0.2, GraphPad Software, San Diego, CA) was used for all statistical analyses. In all cases, $*p < 0.05$, $**p < 0.01$, $***p < 0.001$, and $****p < 0.0001$.

Results

TLR2/6 stimulation, but not TLR1/2 stimulation, is associated with earlier leukemia and death in the NHD13 mice

We previously reported that young adult *NHD13* mice have increased surface TLR2 on their hematopoietic stem and progenitor (c-Kit+Sca-1+Lineage- [KSL]) cells compared with WT littermates [19]. Using flow cytometry, we determined that surface expression of the TLR2 binding partners, TLR1 and TLR6, is also increased on KSL cells of the *NHD13* mice compared with WT littermates (Figure 1A,B; Supplementary Figure E1, online only, available at www.exphem.org). We then asked how chronic exposure to TLR1/2 versus TLR2/6 ligands influences hematopoiesis and disease progression in the *NHD13* mice. To this end, *NHD13* mice and WT littermate controls were treated chronically (three times

weekly) with the TLR1/2 agonist PAM_3CSK_4, the TLR2/6 agonist PAM_2CSK_4, or vehicle (water) alone. We used doses of these agonists that had similar effects on the HSPCs of WT mice (Figure 2A–G) and that also had similar effects on the activation of known downstream targets of TLR2 signaling, including phosphorylation of STAT1 and ERK1/2 (Figure 1C; Supplementary Figure E2, online only, available at www.exphem.org). Long-term treatment with these agonists had minimal effects on WT mice, who exhibited only a modest reduction in platelets with the TLR1/2 agonist (PAM_3CSK_4, Figure 1D–F) and, with the exception of one death in the TLR2/6 agonist (PAM_2CSK_4) cohort from an unknown cause, lived >500 days (at which time they were sacrificed/censored from the study, Figure 1G). Consistent with prior reports [18,19,23], we found reduced white blood cell (WBC) and platelet counts in *NHD13* mice compared with WT controls at baseline. In contrast to WT mice, treatment of *NHD13* mice with the TLR2/6 agonist increased WBC counts in preleukemic mice (Figure 1D), and both agonists further decreased platelet counts (Figure 1F). Notably, treatment of the *NHD13* mice with the TLR2/6 agonist (PAM_2CSK_4), but not the TLR1/2 agonist (PAM_3CSK_4), was associated with earlier death than water treatment alone (Figure 1G). The cause of death for each mouse was determined using flow cytometry and histopathologic evaluation by a hematopathologist (EJD) following the Bethesda criteria [24]. The most common determined cause of death in the *NHD13* mice, including those treated with the TLR2/6 agonist, was leukemia (Figure 1H,I; Supplementary Table E1, online only, available at www.exphem.org). Supporting a role for TLR6 in promoting leukemogenesis, we found that loss of TLR6, but not TLR1, is associated with significantly longer survival in the *NHD13* mice (Supplementary Figure E3 and Supplementary Tables E2 and E3, online only, available at www.exphem.org). In addition, compared with *NHD13* mice, *NHD13;Tlr6*$^{-/-}$ mice more often died of MDS rather than leukemia (Supplementary Figure E3 and Supplementary Table E2). Of note, neither TLR1 nor TLR6 loss affected the peripheral blood counts of *NHD13* mice (Supplementary Figure E3).

TLR2/6 agonist treatment expands premalignant HSPCs

To gain insight into the differential effects of TLR1/2 versus TLR2/6 signaling on survival of the *NHD13* mice, we looked at the effects of the different agonist treatments on the stem and progenitor cell populations (Figure 2A). Specifically, young adult *NHD13* mice and WT littermate controls were treated for 2 weeks with either the TLR1/2 or TLR2/6 agonist (using the same doses and schedule as described for chronic treatment), and HSPC numbers were assessed by flow cytometry. While the different agonists had similar effects on WT mice, increasing both KSL cells and KSL CD150+CD48− (KSL SLAM, or long-term hematopoietic stem cells), the TLR2/6 agonist (PAM_2CSK_4) expanded KSL and KSL SLAM cells in the *NHD13* mice to a significantly greater extent than the TLR1/2 agonist PAM_3CSK_4 (Figure 2B–E; Supplementary Figure E4A, online only, available at www.exphem.org). Of note, myeloid progenitors were expanded in the WT mice in response to the TLR1/2 agonist, but not the TLR2/6 agonist (Supplementary Figure E4B,C). Consistent with the greater expansion of the KSL cells in the *NHD13* mice in response to TLR2/6 agonist treatment, we found a higher percentage of these cells were actively cycling (Figure 2F–H) compared with those of the TLR1/2-agonist treated mice or those from mice treated with water alone. The HSPCs of *NHD13* mice have high rates of cell death [23,25], and this cell death (as measured by Annexin V staining, Figure 2I) is modestly reduced in

the TLR2/6 agonist-treated animals compared with the TLR1/2 agonist-treated ones (with a trending reduction in death compared with water-treated controls). The KSL population from *NHD13* mice has previously been reported to be capable of serial replating in methylcellulose and to contain the transplantable, disease-initiating cells [26–28]. To confirm that the expanded KSL population in the PAM_2CSK_4-treated mice retains these properties, we sorted KSL cells from WT and *NHD13* mice treated for 2 weeks with the TLR1/2 (PAM_3CSK_4) or TLR2/6 (PAM_2CSK_4) agonist, or water alone, and performed serial replatings in MethoCult. Indeed, the KSL cells from TLR2 agonist-treated *NHD13* mice were capable of generating colonies through serial replatings, while the WT KSL cells failed after the third replating (Supplementary Figure E5A, online only, available at www.exphem.org). In addition, sorted KSL cells from TLR2 agonist-treated or control *NHD13* mice were capable of long-term engraftment in sublethally irradiated WT recipient mice, albeit with a predominately Gr-1+ population (Supplementary Figure E5B,C). These findings are similar to those for the cells from water controltreated *NHD13* mice. Thus, TLR2/6 agonist exposure expands premalignant HSPCs in the *NHD13* mice to a greater extent than TLR1/2 agonist treatment, and these expanded cells remain capable of serial replating and long-term repopulation. Finally, to rule out the possibility that off-target effects of the TLR agonists are responsible for HSPC expansion, we treated TLRdeficient mice with PAM_2CSK_4 or PAM_3CSK_4. As expected, the TLR2/6 agonist-mediated expansion is dependent on both TLR2 and TLR6, as no KSL expansion was observed in *NHD13;Tlr2*$^{-/-}$ and *NHD13; Tlr6*$^{-/-}$ mice treated with PAM_2CSK_4. In addition, the more modest expansion of KSL cells in the *NHD13* mice in response to PAM_3CSK_4 is dependent on TLR2 and TLR1 (Figure 2J).

Serum IL-6 levels are increased in response to TLR2/6 agonist exposure

Having found that there are differential effects of TLR2/6 versus TLR1/2 ligand exposure on the KSL cells of *NHD13* mice, we considered that this may be either a direct, cell-autonomous effect of these ligands or an indirect, non-cell-autonomous effect. To distinguish between these possibilities, we first asked whether there were differences in serum cytokine levels (a likely source of indirect effectors of the differential effects of TLR agonists) in mice treated with the TLR1/2 agonist compared with the TLR2/6 agonist. Using a membrane-based antibody array, we profiled 40 serum cytokines in WT and *NHD13* mice following a single dose of PAM_2CSK_4 or PAM_3CSK_4 compared with vehicle. While multiple cytokines were similarly elevated in WT and *NHD13* mice in response to both TLR2 agonists (Figure 3A; Supplementary Figure E6, online only, available at www.exphem.org), three cytokines significantly differed between PAM_2CSK_4 and PAM_3CSK_4 in the *NHD13* mice. IL-3 and IL-4 were slightly, but significantly, higher in the serum of PAM_3CSK_4-treated mice compared with PAM_2CSK_4-treated mice, while IL-6 was markedly higher in the PAM_2CSK_4-treated group (Figure 3A; Supplementary Figure E6). Serum IL-6 levels increased in WT mice in response to PAM_2CSK_4 as well, though not to as great an extent, as in the *NHD13* mice (Figure 3B). We confirmed the robust increase in serum IL-6 in response to PAM_2CSK_4 by enzyme-linked immunosorbent assay (ELISA) and found that even very high doses of PAM_3CSK_4 did not induce IL-6 production to the degree that lower doses of PAM_2CSK_4 did (Figure 3C). Finally, using mice deficient for TLR1, TLR2, or TLR6, we found that the PAM_2CSK_4-induced production of IL-6 is dependent on

both TLR2 and TLR6. Notably, however, the modest increase in serum IL-6 levels in response to PAM_3CSK_4, while dependent on TLR2, does not require TLR1 (Figure 3D).

Loss of IL-6 does not mitigate the effects of TLR2/6 agonist exposure on premalignant HSPCs

To determine whether the effects of PAM_2CSK_4 on HSPC expansion and cycling in the *NHD13* mice are IL-6 dependent, we crossed the *NHD13* mice to mice lacking IL-6. Treatment of these *NHD13;IL-6*$^{-/-}$ mice with a 2-week course of PAM_2CSK_4, as described above, revealed that, similar to those of *NHD13* mice, the HSPCs of *NHD13;IL-6*$^{-/-}$ mice cycled and increased in number in response to TLR2/6 agonist exposure more robustly than in response to the TLR1/2 agonist (Figure 4A–F). Thus, although serum IL-6 is markedly increased in response to PAM_2CSK_4, this cytokine does not appear to be a major player in promoting the expansion of premalignant HSPCs in this context.

Cell autonomous TLR2/6 signaling contributes to the proliferation of premalignant HSPCs in response to TLR2/6 agonist treatment

Given that the proliferation of HSPCs in PAM_2CSK_4-treated *NHD13* mice is not due to indirect effects of IL-6, we next asked whether there is a direct, cell-autonomous effect of TLR2/6 stimulation on HSPCs. To do this, we generated chimeric mice in which a 1:1 mixture of *NHD13* (CD45.1/CD45.2) and *NHD13; Tlr6*$^{-/-}$ or *NHD13;Tlr2*$^{-/-}$ (CD45.2) bone marrow cells were transplanted into lethally irradiated WT (CD45.1) recipients (Figure 5A). After allowing time for engraftment, these chimeric mice were treated with a 2-week course of PAM_2CSK_4 as described above. Analysis of the bone marrow HSPCs of these mice (Figure 5B,C; Supplementary Figure E7, online only, available at www.exphem.org) revealed that the TLR2/6-expressing cells (*NHD13*, CD45.1/CD45.2) increased in frequency and cycled more robustly in response to PAM_2CSK_4 than the *NHD13* cells lacking TLR2 or TLR6 (CD45.2), suggesting that cell-autonomous TLR2/6 contributes to the proliferation of these premalignant HSPCs in response to TLR2/6 agonist treatment.

TLR2/6 agonist treatment is associated with activation of Myc and mTORC1

To further elucidate the mechanism underlying the differential effects of the TLR2/6 and TLR1/2 agonists on HSPC expansion and cycling, we sorted KSL cells from young adult *NHD13* mice and WT littermate controls treated for 2 weeks with PAM_2CSK_4, PAM_3CSK_4, or water alone as described above and performed RNA expression analysis. Notably, GSEA identified Myc and mTORC1 activation among the top most highly enriched pathways in both WT and *NHD13* HSPCs treated with PAM_2CSK_4 compared with PAM_3CSK_4 (Figure 6A; Supplementary Figure E8, online only, available at www.exphem.org). To determine the contribution of these pathways to the expansion of premalignant HSPCs in response to TLR2/6 stimulation, we treated *NHD13* mice with either the BET bromodomain inhibitor JQ1, which reduces Myc activity [29], or the mTORC1 inhibitor rapamycin [30], in conjunction with PAM_2CSK_4 or PAM_3CSK_4. In doing this, we found that JQ1 treatment led to a trend toward a reduction in PAM_2CSK_4-induced HSPC expansion, and conversely, rapamycin exacerbated this expansion (Figure 6B–D). Neither inhibitor significantly influenced the effects of PAM_3CSK_4 on premalignant HSPCs. Furthermore, rapamycin did

not significantly affect the PAM_2CSK_4-induced expansion of KSL cells in WT mice, suggesting that its effects are unique to the premalignant HSPCs (Figure 6E,F).

Discussion

We previously reported that complete loss of TLR2 signaling accelerates disease progression in *NHD13* mice [19], suggesting that TLR2, whose expression correlates with lower-risk MDS [3,11], may play a protective role against leukemic transformation. In this study, we aimed to elucidate heterodimer-specific effects of TLR2 signaling in this model. TLR2 functions in partnership with either TLR1 or TLR6, and unlike those of TLR2, TLR6 (though not TLR1) levels have been reported to correlate with higher-risk disease [3], suggesting that there may be differential effects of TLR1/2 versus TLR2/6 signaling in MDS. Indeed, we found that TLR2/6, but not TLR1/2, stimulation exacerbates disease progression and promotes the expansion of premalignant HSPCs, while loss of TLR6 leads to longer survival. This suggests that while preservation of some TLR2-mediated signaling may be protective against transformation in higher-risk MDS, inhibition of TLR6-mediated signaling specifically may be beneficial in slowing this process.

Intriguingly, we found that serum IL-6 levels are much more robustly increased with TLR2/6 stimulation compared with TLR1/2 stimulation. This increase in IL-6 may account for the differential effects of the TLR2 agonists on platelet numbers in WT mice [31], which were significantly higher in the PAM_2CSK_4-treated compared with PAM_3CSK_4-treated mice. However, the expansion of premalignant HSPCs in response to PAM_2CSK_4 treatment is not dependent on IL-6. Rather, our chimeric mouse studies suggest that this expansion is, at least in part, due to cell-autonomous TLR2/6 signaling, as cycling and expansion in response to PAM_2CSK_4 occurred more robustly in the HSPCs that expressed TLR2/6 compared with those that did not. As TLR1, TLR2, and TLR6 are all expressed on HSPCs, it is not clear why their responses to TLR1/2 and TLR2/6 stimulation are different. As discussed below, GSEA suggested a more robust activation of mTORC1 and Myc in response to TLR2/6 ligation, and further studies are needed to determine the signaling differences in the HSPCs in response to the different TLR2 ligands that might account for the differential activation of these targets. While TLR1/2 and TLR2/6 heterodimers recognize unique ligands, their downstream signaling is thought to be very similar, with both heterodimers acting through the adaptor MyD88 to ultimately activate NF-κB, MAPK, and PI3K pathways [32]. However, our understanding of the heterodimer-specific signaling is incomplete, and previous reports have suggested that, indeed, the kinetics of activation of these pathways differs between TLR1/2 and TLR2/6 stimulation [33]. Further studies are necessary to better elucidate how ligation of these specific heterodimers influences downstream signaling in both normal and premalignant HSPCs.

As noted above, our RNA profiling studies suggested activation of mTORC1 and Myc in response to TLR2/6 agonist treatment. Activation of both mTORC1 and Myc have been described in patients with MDS [34,35], and both are known regulators of normal, premalignant, and malignant HSPCs; however, the connection between these pathways and TLR signaling in MDS is not known. mTORC1 is a protein complex involved in the regulation of protein translation and cellular metabolism [36,37]. Activation of mTORC1 by

TLR ligands has been described previously, though not specifically in HSPCs. For example, Lorne and colleagues [38] reported that mTORC1 activation in response to TLR2 or TLR4 ligands was necessary for optimal cellular activation and cytokine production in neutrophils. In addition, TLR2 signaling has been found to activate mTORC1 in regulatory T cells, promoting glucose transport and cell proliferation [39]. Although the role of mTORC1 in response to TLR ligation in HSPCs in particular has not been described, mTORC1 is a known regulator of HSPC function. Specifically, aberrant activation of mTORC1 leads to a loss of HSC quiescence and reduced self-renewal capacity [40,41]. Somewhat surprisingly, then, we found that inhibition of mTORC1 with rapamycin exacerbated the TLR2/6 agonist-mediated cycling and expansion of premalignant HSPCs in the *NHD13* mice. However, in addition to its growth-promoting properties, mTORC1 has been reported to serve an immunomodulatory role in response to inflammatory and infectious stimuli, dampening the cytokine response of certain immune effector cells in response to such stimuli [42–44]. Further studies are necessary to elucidate the mechanism of the exacerbated TLR2/6 agonist response of premalignant HSPCs with mTORC1 inhibition. In contrast to mTORC1 inhibition, suppression of Myc using the bromodomain inhibitor JQ1 led to a trend in reduction of the TLR2/6-mediated expansion of premalignant HSPCs. Myc is a proto-oncogene whose expression correlates with higher-risk MDS, and Myc has been previously implicated in promoting cell proliferation in response to TLR signaling [45,46]. Additional studies are needed to understand the effects of Myc and mTORC1 modulation on premalignant HSPC function in the context of TLR2 agonist stimulation, as well as to determine whether similar effects on premalignant HSPCs are seen in other MDS models.

Together, our data suggest the presence of unique heterodimer-specific effects of TLR2 signaling on premalignant HSPCs, and these effects are, at least in part, cell autonomous, with TLR2/6 stimulation promoting cell cycling and leading to faster leukemic transformation and death in the *NHD13* mice. TLR6, therefore, may represent a promising therapeutic target in patients with elevated expression. Ongoing studies are aimed at better understanding how TLR2/6 signaling uniquely promotes premalignant HSPC expansion and the role that mTORC1 and Myc play in this process.

Supplementary Material

Refer to Web version on PubMed Central for supplementary material.

Acknowledgments

We thank the Alvin J. Siteman Cancer Center at Washington University School of Medicine and Barnes-Jewish Hospital for the use of the Siteman Flow Cytometry Core. We thank Jackie Tucker-Davis, Alex Sorensen, and Patrick Shumway for animal care. We thank John Keller, Nate Roundy, and Dagmar Ralphs for technical assistance. We thank the Genome Technology Access Center at Washington University School of Medicine and Wei Yang for RNA profiling services.

This work was supported by grants from the Children's Discovery Institute of Washington University and St. Louis Children's Hospital (LGS), the Washington University SPORE in Leukemia's Career Enhancement Program (LGS), the American Cancer Society (RSG-17-166-01-DCC [LGS]), and the National Heart, Lung, and Blood Institute (1R01 HL134896-01 [LGS]).

References

1. Jacobs A Myelodysplastic syndromes: pathogenesis, functional abnormalities, and clinical implications. J Clin Pathol. 1985; 38:1201–1217. [PubMed: 2999194]
2. Galton DA. The myelodysplastic syndromes. Clin Lab Haematol. 1984;6:99–112. [PubMed: 6386287]
3. Wei Y, Dimicoli S, Bueso-Ramos C, et al. Toll-like receptor alterations in myelodysplastic syndrome. Leukemia. 2013;27:1832–1840. [PubMed: 23765228]
4. Starczynowski DT, Kuchenbauer F, Argiropoulos B, et al. Identification of miR-145 and miR-146a as mediators of the 5q– syndrome phenotype. Nat Med. 2010;16:49–58. [PubMed: 19898489]
5. Dimicoli S, Wei Y, Bueso-Ramos C, et al. Overexpression of the toll-like receptor (TLR) signaling adaptor MYD88, but lack of genetic mutation, in myelodysplastic syndromes. PLoS One. 2013;8:e71120. [PubMed: 23976989]
6. Maratheftis CI, Andreakos E, Moutsopoulos HM, Voulgarelis M. Toll-like receptor-4 is up-regulated in hematopoietic progenitor cells and contributes to increased apoptosis in myelodysplastic syndromes. Clin Cancer Res. 2007;13:1154–1160. [PubMed: 17317824]
7. Velegraki M, Papakonstanti E, Mavroudi I, et al. Impaired clearance of apoptotic cells leads to HMGB1 release in the bone marrow of patients with myelodysplastic syndromes and induces TLR4-mediated cytokine production. Haematologica. 2013; 98:1206–1215. [PubMed: 23403315]
8. Varney ME, Niederkorn M, Konno H, et al. Loss of Tifab, a del (5q) MDS gene, alters hematopoiesis through derepression of Toll-like receptor-TRAF6 signaling. J Exp Med. 2015;212:1967–1985. [PubMed: 26458771]
9. Varney ME, Melgar K, Niederkorn M, Smith MA, Barreyro L, Starczynowski DT. Deconstructing innate immune signaling in myelodysplastic syndromes. Exp Hematol. 2015;43:587–598. [PubMed: 26143580]
10. Monlish DA, Bhatt ST, Schuettpelz LG. The role of toll-like receptors in hematopoietic malignancies. Front Immunol. 2016;7:390. [PubMed: 27733853]
11. Zeng Q, Shu J, Hu Q, et al. Apoptosis in human myelodysplastic syndrome CD34+ cells is modulated by the upregulation of TLRs and histone H4 acetylation via a beta-arrestin 1 dependent mechanism. Exp Cell Res. 2016;340:22–31. [PubMed: 26708616]
12. Sallman DA, Cluzeau T, Basiorka AA, List A. Unraveling the pathogenesis of MDS: the NLRP3 inflammasome and pyroptosis drive the MDS phenotype. Front Oncol. 2016;6:151. [PubMed: 27379212]
13. Esplin BL, Shimazu T, Welner RS, et al. Chronic exposure to a TLR ligand injures hematopoietic stem cells. J Immunol. 2011;186:5367–5375. [PubMed: 21441445]
14. Herman AC, Monlish DA, Romine MP, Bhatt ST, Zippel S, Schuettpelz LG. Systemic TLR2 agonist exposure regulates hematopoietic stem cells via cell-autonomous and cell-non-autonomous mechanisms. Blood Cancer J. 2016;6:e437. [PubMed: 27315114]
15. Takizawa H, Fritsch K, Kovtonyuk LV, et al. Pathogen-induced TLR4-TRIF innate immune signaling in hematopoietic stem cells promotes proliferation but reduces competitive fitness. Cell Stem Cell. 2017;21:225–240. e225. [PubMed: 28736216]
16. Zhang H, Rodriguez S, Wang L, et al. Sepsis induces hematopoietic stem cell exhaustion and myelosuppression through distinct contributions of TRIF and MYD88. Stem Cell Rep. 2016;6:940–956.
17. Gil-Perez A, Montalban-Bravo G. Management of myelodysplastic syndromes after failure of response to hypomethylating agents. Ther Adv Hematol. 2019;10:2040620719847059. [PubMed: 31156799]
18. Lin YW, Slape C, Zhang Z, Aplan PD. NUP98-HOXD13 transgenic mice develop a highly penetrant, severe myelodysplastic syndrome that progresses to acute leukemia. Blood. 2005;106:287–295. [PubMed: 15755899]
19. Monlish DA, Bhatt ST, Duncavage EJ, et al. Loss of Toll-like receptor 2 results in accelerated leukemogenesis in the NUP98-HOXD13 mouse model of MDS. Blood. 2018;131:1032–1035. [PubMed: 29358180]

20. Belkina AC, Nikolajczyk BS, Denis GV. BET protein function is required for inflammation: Brd2 genetic disruption and BET inhibitor JQ1 impair mouse macrophage inflammatory responses. J Immunol. 2013;190:3670–3678. [PubMed: 23420887]
21. Amend SR, Valkenburg KC, Pienta KJ. Murine hind limb long bone dissection and bone marrow isolation. J Vis Exp. 2016; 110:53936.
22. Schuettpelz LG, Gopalan PK, Giuste FO, Romine MP, van Os R, Link DC. Kruppel-like factor 7 overexpression suppresses hematopoietic stem and progenitor cell function. Blood. 2012; 120:2981–2989. [PubMed: 22936656]
23. Slape CI, Saw J, Jowett JB, et al. Inhibition of apoptosis by BCL2 prevents leukemic transformation of a murine myelodysplastic syndrome. Blood. 2012;120:2475–2483. [PubMed: 22855610]
24. Kogan SC, Ward JM, Anver MR, et al. Bethesda proposals for classification of nonlymphoid hematopoietic neoplasms in mice. Blood. 2002;100:238–245. [PubMed: 12070033]
25. Choi CW, Chung YJ, Slape C, Aplan PD. Impaired differentiation and apoptosis of hematopoietic precursors in a mouse model of myelodysplastic syndrome. Haematologica. 2008;93:1394–1397. [PubMed: 18603548]
26. Cheng G, Liu F, Asai T, et al. Loss of p300 accelerates MDSassociated leukemogenesis. Leukemia. 2017;31:1382–1390. [PubMed: 27881875]
27. Chung YJ, Choi CW, Slape C, Fry T, Aplan PD. Transplantation of a myelodysplastic syndrome by a long-term repopulating hematopoietic cell. Proc Natl Acad Sci USA. 2008;105:14088–14093. [PubMed: 18768819]
28. Guirguis AA, Slape CI, Failla LM, et al. PUMA promotes apoptosis of hematopoietic progenitors driving leukemic progression in a mouse model of myelodysplasia. Cell Death Differ. 2016;23:1049–1059. [PubMed: 26742432]
29. Mertz JA, Conery AR, Bryant BM, et al. Targeting MYC dependence in cancer by inhibiting BET bromodomains. Proc Natl Acad Sci USA. 2011;108:16669–16674. [PubMed: 21949397]
30. Heitman J, Movva NR, Hall MN. Targets for cell cycle arrest by the immunosuppressant rapamycin in yeast. Science. 1991;253:905–909. [PubMed: 1715094]
31. Ishibashi T, Kimura H, Shikama Y, et al. Interleukin-6 is a potent thrombopoietic factor in vivo in mice. Blood. 1989; 74:1241–1244. [PubMed: 2788464]
32. Farhat K, Riekenberg S, Heine H, et al. Heterodimerization of TLR2 with TLR1 or TLR6 expands the ligand spectrum but does not lead to differential signaling. J Leukoc Biol. 2008;83:692–701. [PubMed: 18056480]
33. Rolf N, Kariminia A, Ivison S, Reid GS, Schultz KR. Hetero-dimer-specific TLR2 stimulation results in divergent functional outcomes in B-cell precursor acute lymphoblastic leukemia. Eur J Immunol. 2015;45:1980–1990. [PubMed: 25867213]
34. Poloni A, Serrani F, Berardinelli E, et al. Telomere length, c-myc and mad-1 expression could represent prognosis markers of myelodysplastic syndrome. Leuk Res. 2013;37:1538–1544. [PubMed: 24095110]
35. Follo MY, Mongiorgi S, Bosi C, et al. The Akt/mammalian target of rapamycin signal transduction pathway is activated in high-risk myelodysplastic syndromes and influences cell survival and proliferation. Cancer Res. 2007;67:4287–4294. [PubMed: 17483341]
36. Loewith R, Jacinto E, Wullschleger S, et al. Two TOR complexes, only one of which is rapamycin sensitive, have distinct roles in cell growth control. Mol Cell. 2002;10:457–468. [PubMed: 12408816]
37. Kim J, Guan KL. mTOR as a central hub of nutrient signalling and cell growth. Nat Cell Biol. 2019;21:63–71. [PubMed: 30602761]
38. Lorne E, Zhao X, Zmijewski JW, et al. Participation of mammalian target of rapamycin complex 1 in Toll-like receptor 2- and 4-induced neutrophil activation and acute lung injury. Am J Respir Cell Mol Biol. 2009;41:237–245. [PubMed: 19131641]
39. Gerriets VA, Kishton RJ, Johnson MO, et al. Foxp3 and Toll-like receptor signaling balance Treg cell anabolic metabolism for suppression. Nat Immunol. 2016;17:1459–1466. [PubMed: 27695003]

40. Ghosh J, Kapur R. Role of mTORC1-S6K1 signaling pathway in regulation of hematopoietic stem cell and acute myeloid leukemia. Exp Hematol. 2017;50:13–21. [PubMed: 28342808]

41. Gan B, DePinho RA. mTORC1 signaling governs hematopoietic stem cell quiescence. Cell Cycle. 2009;8:1003–1006. [PubMed: 19270523]

42. Weichhart T, Costantino G, Poglitsch M, et al. The TSC-mTOR signaling pathway regulates the innate inflammatory response. Immunity. 2008;29:565–577. [PubMed: 18848473]

43. Ohtani M, Nagai S, Kondo S, et al. Mammalian target of rapamycin and glycogen synthase kinase 3 differentially regulate lipopolysaccharide-induced interleukin-12 production in dendritic cells. Blood. 2008;112:635–643. [PubMed: 18492954]

44. Weichhart T, Hengstschlager M, Linke M. Regulation of innate immune cell function by mTOR. Nat Rev Immunol. 2015;15:599–614. [PubMed: 26403194]

45. Pries R, Hogrefe L, Xie L, et al. Induction of c-Myc-dependent cell proliferation through toll-like receptor 3 in head and neck cancer. Int J Mol Med. 2008;21:209–215. [PubMed: 18204787]

46. Lee SH, Hu LL, Gonzalez-Navajas J, et al. ERK activation drives intestinal tumorigenesis in Apc(min/+) mice. Nat Med. 2010;16:665–670. [PubMed: 20473309]

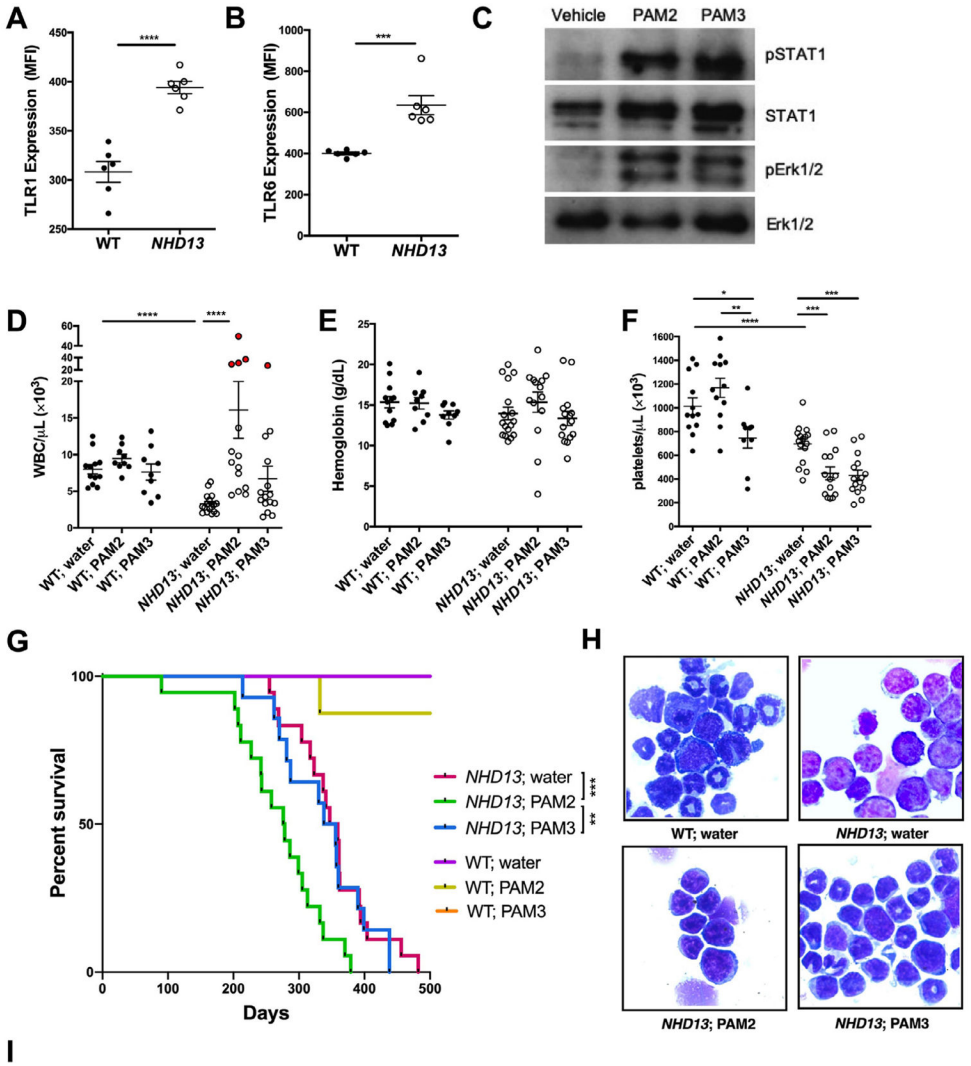

I

	NHD13			Wild-Type		
Cause of Death	Water	PAM2CSK4	PAM3CSK4	Water	PAM2CSK4	PAM3CSK4
Leukemia	5	6	4			
MPD-like Leukemia	1	1	6			
MDS	1					
Unknown	11	11	4		1	

Figure 1.

TLR2/6 stimulation, but not TLR1/2 stimulation, is associated with earlier leukemia and death in *NHD13* mice. Surface expression of TLR1 (**A**) and TLR6 (**B**) on c-Kit +Sca-1+Lineage− (KSL) cells of WT and *NHD13* mice (age 6–8 weeks) is depicted; data represent the median fluorescent intensity as determined by flow cytometry (see Supplementary Figure E1 for representative gating). (**C**–**I**) *NHD13* mice or WT littermates were treated chronically (3 × weekly IP injections) with the TLR1/2 agonist PAM_3CSK_4 (25 μg/dose) or the TLR2/6 agonist PAM_2CSK_4 (1 μg/dose) starting at 8 weeks of age. (**C**) Western blot of 30,000 sorted KSL cells from WT mice treated with the indicated agonists, showing total and phosphorylated STAT1 and Erk1/2. (**D**–**F**) Peripheral blood WBCs (**D**), hemoglobin (**E**), and platelets (**F**) of mice at 5 months of age are shown for each treatment

group. Note that some mice already had evidence of leukemia at this time point (*red dots* in **D**), and were left out of the statistical calculations for WBCs. (**G**) Kaplan-Meier survival curves of WT and *NHD13* mice treated with the different TLR2 agonists or vehicle (water) alone. (**H**) Representative cytospins from the bone marrow revealing normal morphology (top left panel, WT mouse, water treated), leukemia (top right panel, *NHD13* mouse, water treated, and bottom left panel, *NHD13* mouse, PAM_2CSK_4 treated) and MPD-like leukemia (bottom right panel, *NHD13* mouse, PAM_3CSK_4-treated). (**I**) The cause of death for each mouse, as indicated, was determined by review of morphology and flow cytometry. See Supplementary Table E1 for more information. *$p < 0.05$, **$p < 0.01$, ***$p < 0.001$, ****$p < 0.0001$ by unpaired Student *t* test or Log-rank (Mantel-Cox) test. Error bars represent the mean ± SEM.

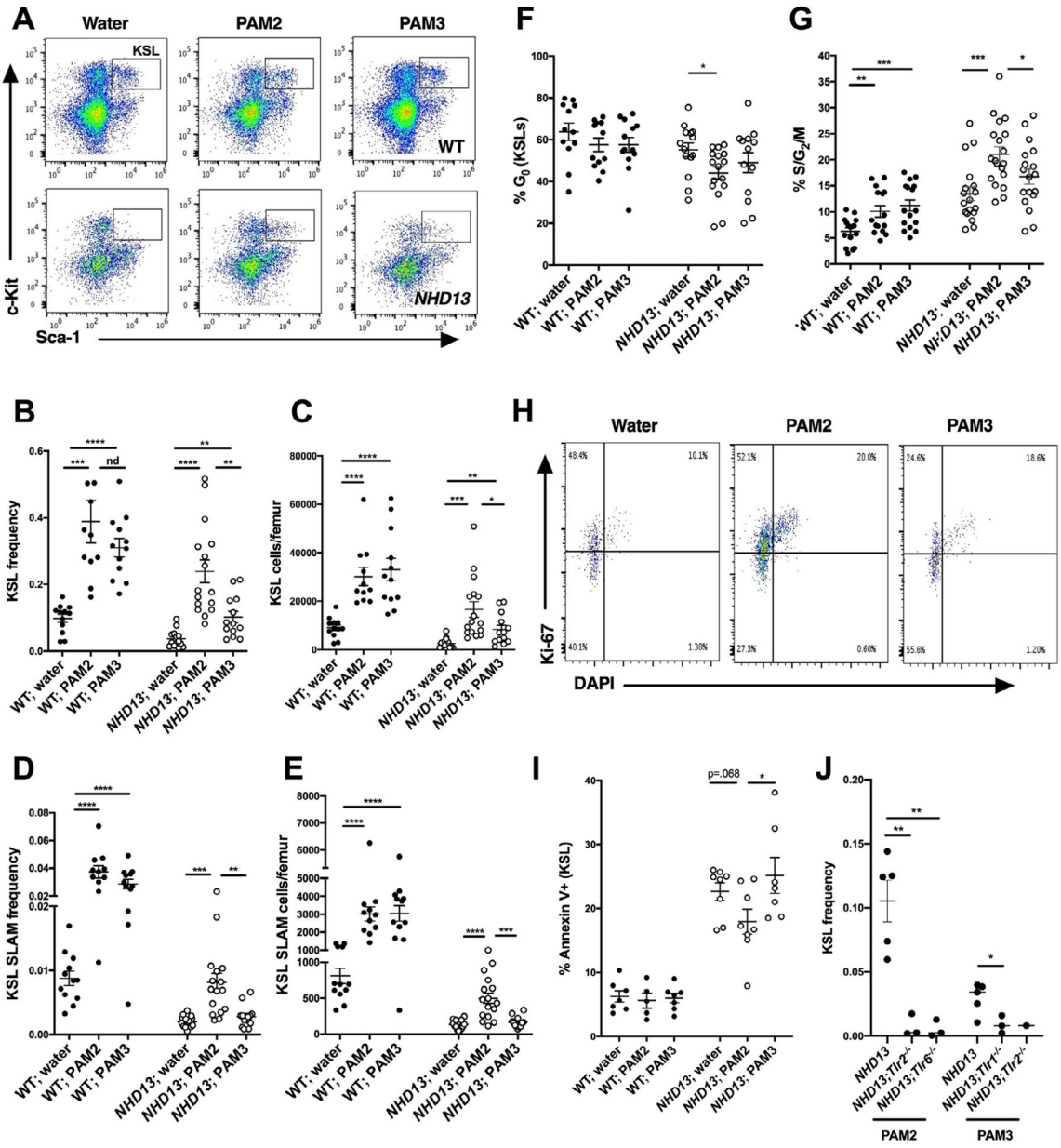

Figure 2.

TLR2/6 agonist treatment expands premalignant HSPCs. (**A**) Young adult (6- to 8-week) *NHD13* mice or WT littermates were treated with a 2-week course (six doses total) of TLR2/6 agonist (PAM_2CSK_4, 1 μg/dose) or TLR1/2 agonist (PAM_3CSK_4, 25 μg/dose), and bone marrow was analyzed by flow cytometry. Shown are representative flow plots of the c-Kit+Sca-1+Lineage− (KSL) cells from the different treatment groups. The frequency among whole bone marrow cells (**B**) and total numbers (**C**) of KSL cells in the bone marrow of the different groups, as well as the frequency (**D**) and total numbers (**E**) of long-term HSCs (Lineage-c-Kit+Sca-1+CD150+CD48− [KSL SLAM] cells) are shown (see Supplementary Figure E3 for representative gating). Percentages of KSL cells in G0 (**F**) and S/G2/M (**G**) of the cell cycle as determined by Ki-67 and DAPI staining. (**H**) Representative Ki-67 and

DAPI staining of KSL cells from water-, PAM_2CSK_4-, and PAM_3CSK_4-treated *NHD13* mice. (**I**) Annexin V staining of KSL cells from the indicated groups. (**J**) *NHD13* mice were crossed to *Tlr1*$^{-/-}$, *Tlr2*$^{-/-}$, or *Tlr6*$^{-/-}$ mice, as indicated, and treated with PAM_2CSK_4 or PAM_3CSK_4 as indicated for 6 doses as above. Shown are the frequencies of KSL cells in the indicated groups. *$p < 0.05$, **$p < 0.01$, ***$p < 0.001$, ****$p < 0.0001$, nd = no statistical difference by unpaired Student *t* test. Error bars represent the mean ± EM.

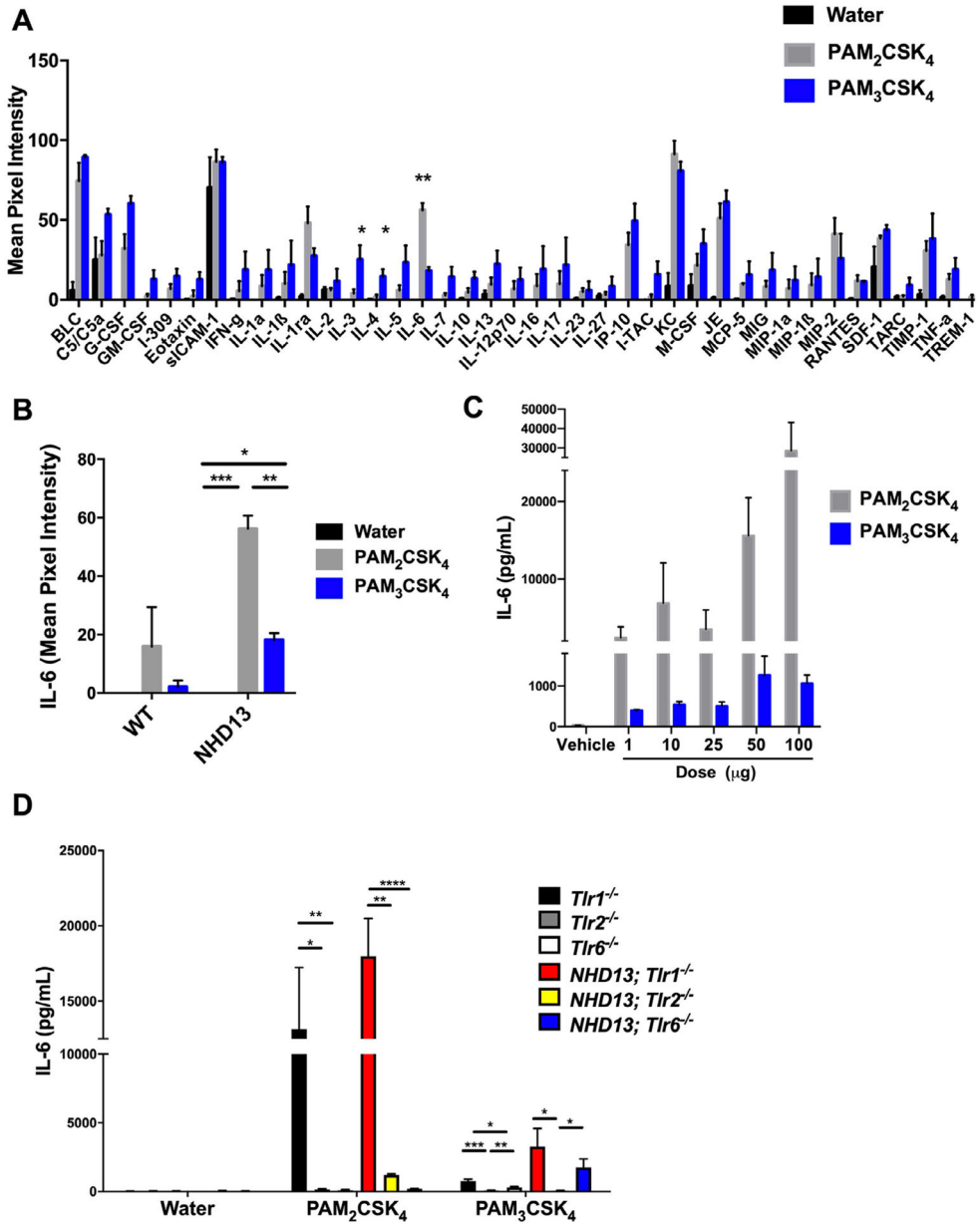

Figure 3.

Serum IL-6 levels are increased in response to TLR2/6 agonist. (**A**) Young adult (6- to 8-week) wild-type (WT) and *NHD13* mice were treated with a single dose of PAM_2CSK_4 (25 μg IP), PAM_3CSK_4 (100 μg IP), or water alone, and serum cytokine levels were measured using a membrane-based antibody array 4 hours later. Membranes were exposed to X-ray film, and signal intensities were quantified for each cytokine. Shown are levels of the indicated cytokines for the *NHD13* mice (n = 3 or 4 independent mice per group; see Supplementary Figure E5 for WT levels and representative blots). (**B**) IL-6 levels as measured in (**A**) are shown for both WT and *NHD13* mice treated with water, PAM_2CSK_4, or PAM_3CSK_4. (**C**) WT mice were treated with increasing doses of PAM_2CSK_4 or PAM_3CSK_4, or water (vehicle) alone, as indicated, and serum IL-6 levels were determined

by ELISA 4 hours later (n = 2 mice/group). (**D**) Mice of the indicated genotypes were given a single dose of PAM_2CSK_4 (25 μg IP), PAM_3CSK_4 (100 μg IP), or water, and serum IL-6 levels were determined by ELISA 4 hours later (n = 2–9 mice/group). *$p < 0.05$, **$p < 0.01$, ***$p < 0.001$, by an unpaired Student t test. Error bars represent mean ± standard error of the mean.

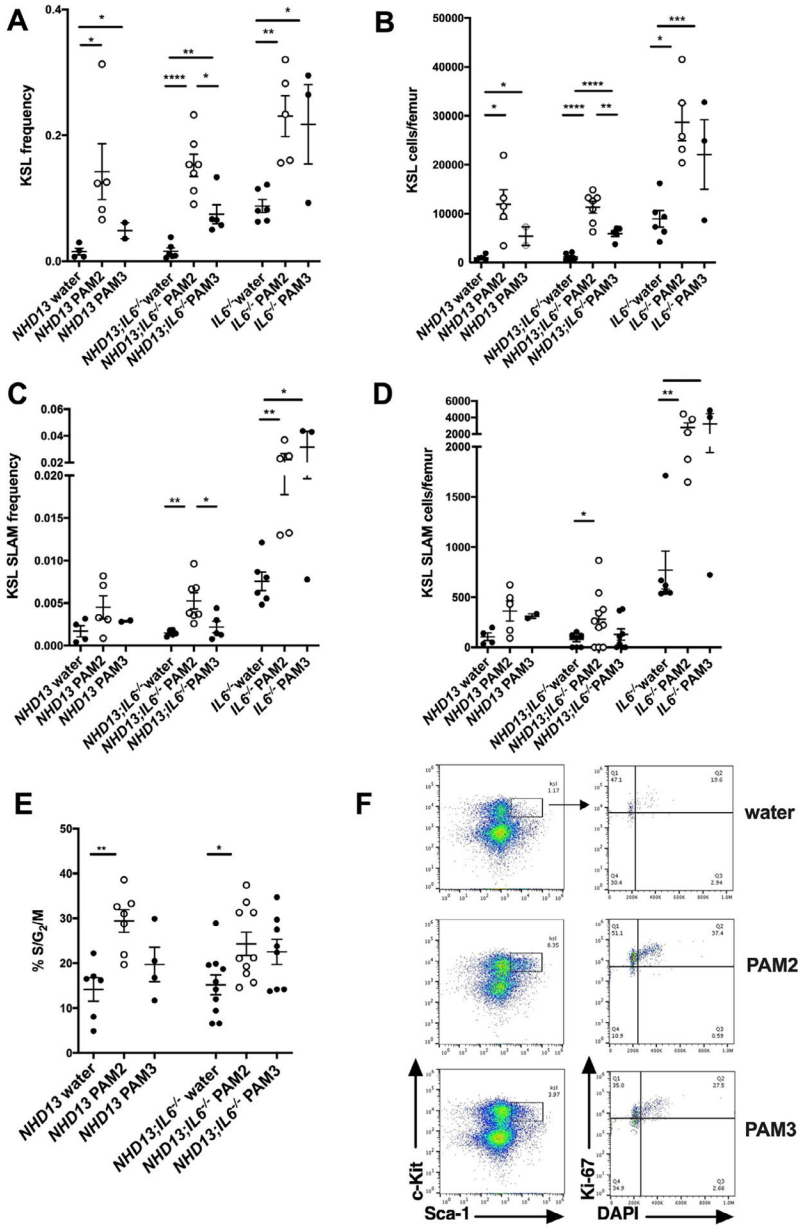

Figure 4.

Loss of IL-6 does not mitigate the expansion of HSPCs in response to TLR2/6 stimulation. Young adult (6- to 8-week-old) *NHD13*, *NHD13;IL-6*$^{-/-}$, or *IL-6*$^{-/-}$ mice were treated with a 2-week course (six doses total) of TLR2/6 agonist (PAM_2CSK_4, 1 μg/dose) or TLR1/2 agonist (PAM_3CSK_4, 25 μg/dose) as for Figure 2, and bone marrow was analyzed by flow cytometry. The frequency (**A**) and total numbers (**B**) of KSL cells in the bone marrow of the different groups, as well as the frequency (**C**) and total numbers (**D**) of KSL SLAM cells are shown. The percentage of KSL cells in S/G2/M (**E**) of the cell cycle as determined by Ki-67 and DAPI staining are shown. (**F**) Shown are representative flow plots of the Ki-67 and DAPI staining of KSL cells from the different treatment groups for the *NHD13;IL-6*$^{-/-}$

mice. *$p < 0.05$, **$p < 0.01$, ***$p < 0.001$, ****$p < 0.0001$ by an unpaired Student t test. Error bars represent the mean ± SEM.

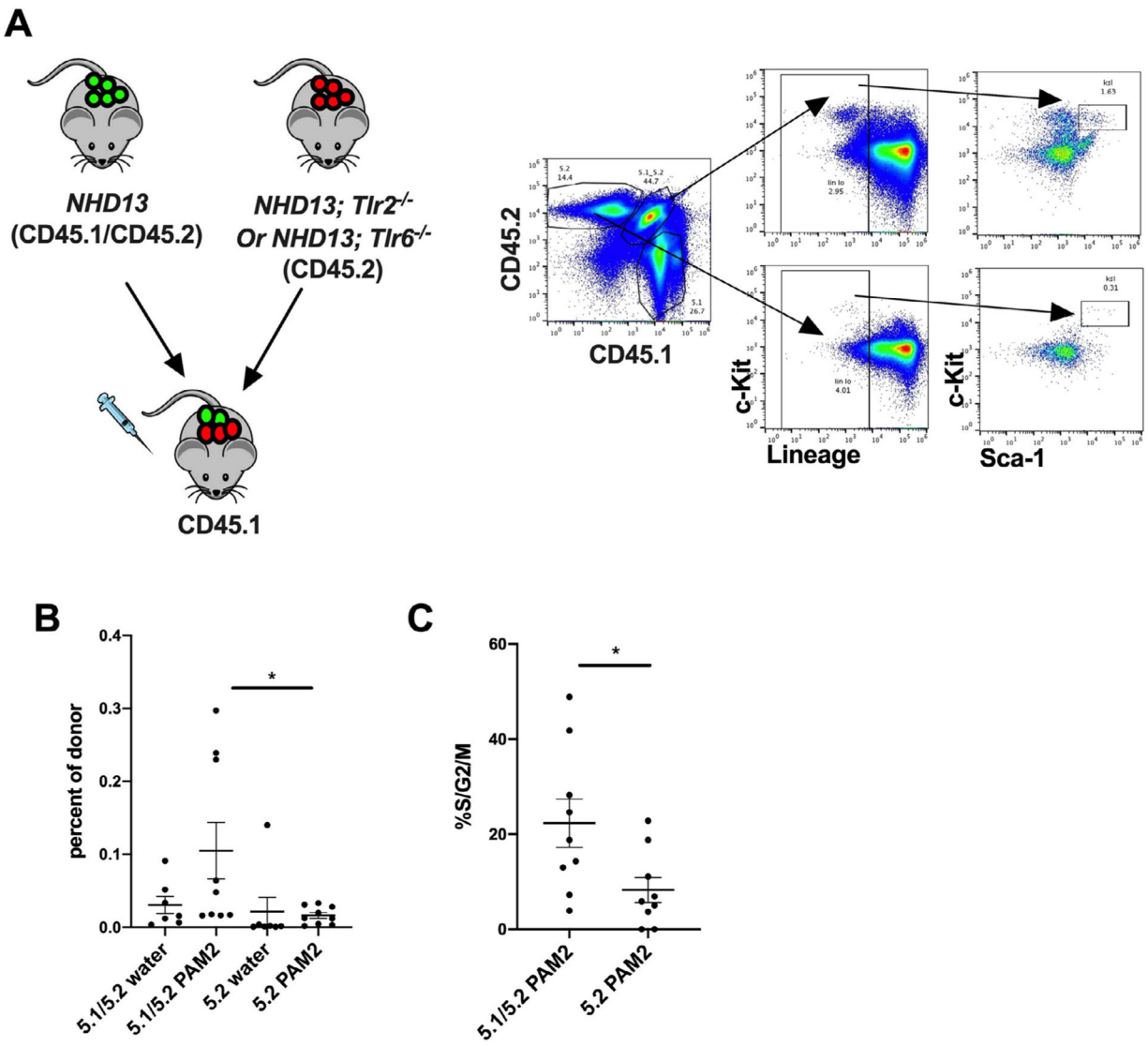

Figure 5.

The TLR2/6 agonist-mediated expansion of HSPCs is, at least in part, cell autonomous. (**A**) Mixed chimeras were generated by mixing bone marrow from *NHD13* mice (generated via crossing *NHD13* (CD45.2) mice with C57BL/6 (B6.SJL-Ptprc* Pep3b BoyJ) mice to generate CD45.1/CD45.2 *NHD13* mice) in a 1:1 ratio with bone marrow from *NHD13;Tlr2*$^{-/-}$ or *NHD13;Tlr6*$^{-/-}$ mice (CD45.2) and transplanting into lethally irradiated WT (B6.SJL-Ptprc* Pep3b BoyJ;CD45.1) recipients. After allowing time for engraftment (>12 weeks), chimeras were treated with PAM_2CSK_4 for 2 weeks, as described above, and their bone marrow was analyzed by flow cytometry. A representative flow plot of *NHD13* (CD45.1/CD45.2) and *NHD13;Tlr2*$^{-/-}$ (CD45.2) KSL cells in a PAM_2CSK_4-treated chimera is shown. (**B**) Frequencies of KSL cells within the indicated donor populations. (**C**) The cycling status of the KSL cells was determined using Ki-67 and DAPI. Shown are the percentage of KSL cells of each genotype in cycle (S/G2/M) from the PAM_2CSK_4-treated chimeras. (Note: similar results were obtained for the *NHD13;Tlr2*$^{-/-}$ and *NHD13;Tlr6*$^{-/-}$

cells, and they are included together as a single group for these analyses. See Supplementary Figure E7 for separated data). *$p < 0.05$ by an unpaired Student t test. Error bars represent the mean ± SEM.

A

Enriched in NHD13 PAM2 vs NHD13 PAM3	NES	NOM p-val	FDR q-val
HALLMARK_MYC_TARGETS_V2	-1.74	0	0.055
HALLMARK_UNFOLDED_PROTEIN_RESPONSE	-1.41	0.054	0.523
HALLMARK_MYC_TARGETS_V1	-1.32	0.128	0.583
HALLMARK_MTORC1_SIGNALING	-1.19	0.269	0.747
HALLMARK_ESTROGEN_RESPONSE_EARLY	-1.09	0.394	0.906
HALLMARK_UV_RESPONSE_UP	-1.06	0.372	0.839
HALLMARK_ESTROGEN_RESPONSE_LATE	-0.97	0.565	0.978
HALLMARK_GLYCOLYSIS	-0.9	0.622	1
HALLMARK_APICAL_SURFACE	-0.84	0.715	1
HALLMARK_FATTY_ACID_METABOLISM	-0.69	0.867	1

Enriched in WT PAM2 vs WT PAM3	NES	NOM p-val	FDR q-val
HALLMARK_MYC_TARGETS_V2	-1.6	0.044	0.504
HALLMARK_PI3K_AKT_MTOR_SIGNALING	-1.56	0	0.355
HALLMARK_OXIDATIVE_PHOSPHORYLATION	-1.55	0.05	0.257
HALLMARK_MYC_TARGETS_V1	-1.54	0.152	0.219
HALLMARK_MTORC1_SIGNALING	-1.54	0.04	0.189
HALLMARK_UNFOLDED_PROTEIN_RESPONSE	-1.52	0	0.201
HALLMARK_ADIPOGENESIS	-1.43	0	0.333
HALLMARK_ANDROGEN_RESPONSE	-1.42	0.069	0.311
HALLMARK_DNA_REPAIR	-1.38	0.081	0.34
HALLMARK_GLYCOLYSIS	-1.38	0.031	0.311

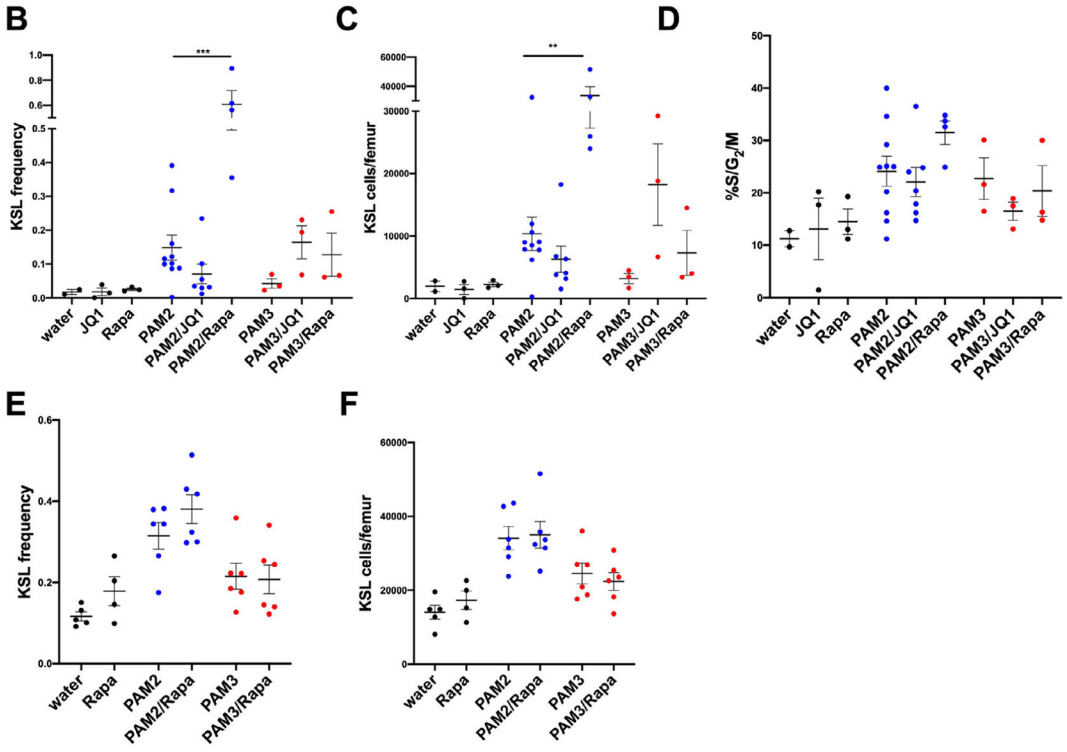

Figure 6.

TLR2/6 agonist treatment is associated with Myc and mTORC1 activation in HSPCs. (**A**) RNA expression arrays were run on sorted KSL cells from WT and *NHD13* mice treated with a 2-week course of PAM_3CSK_4, PAM_2CSK_4, or water alone. Shown are the most significantly enriched Hallmark gene sets comparing PAM_2CSK_4- with PAM_3CKS_4-treated cells from *NHD13* and WT mice. *NHD13* mice were treated with the bromodomain inhibitor JQ1 (which inhibits Myc) or the mTORC1 inhibitor rapamycin. Shown are the frequency (**B**), absolute numbers (**C**), and cycling status (**D**) of KSL cells from *NHD13* mice following treatment with the inhibitors alone, PAM_2CSK_4 alone, PAM_3CSK_4 alone, or the combinations as indicated. (**E**,**F**) WT mice were treated with rapamycin, PAM_2CSK_4 alone, PAM_3CSK_4 alone, or the combinations as indicated. Shown are the frequency (**E**) and

absolute numbers (**F**) of KSL cells in the bone marrow following treatment. $^{**}p < 0.01$, $^{***}p < 0.001$, by unpaired Student *t* test. Error bars represent the mean ± SEM.